

Hamilton-Jacobi method for molecular distribution function in a chemical oscillator

Hiizu Nakanishi and Takahiro Sakaue

Department of Physics, Kyushu University 33, Fukuoka 812-8581, Japan

Jun'ichi Wakou

Miyakonojo National College of Technology,

Miyakonojo-shi, Miyazaki, 885-8567, Japan.

(Dated: July 2, 2018)

Abstract

Using the Hamilton-Jacobi method, we solve chemical Fokker-Planck equations within the Gaussian approximation and obtain a simple and compact formula for a conditional probability distribution. The formula holds in general transient situations, and can be applied not only for a steady state but also for a oscillatory state. By analyzing the long time behavior of the solution in the oscillatory case, we obtain the phase diffusion constant along the periodic orbit and the steady distribution perpendicular to it. A simple method for numerical evaluation of these formulas are devised, and they are compared with Monte Carlo simulations in the case of Brusselator as an example. Some results are shown to be identical to previously obtained expressions.

PACS numbers: 83.80.Hj, 83.60.Rs, 83.10.Ff, 83.60.Wc

I. INTRODUCTION

Chemical reactions are molecular processes and subject to the molecular fluctuations. Such fluctuations are negligible in homogeneous macroscopic systems and the rate equation description is precise enough. However, as the number of molecules involved decreases, the fluctuations become visible and the system behavior may be quite different from the one expected from the rate equation, especially in non-equilibrium systems that show chemical oscillation, bifurcation, bistability, etc.

The study on stochasticity in chemical reactions has a long history as a fundamental problem of irreversible statistical physics[1–3], but its interests remained largely academic until recently because experimental observations were limited. However, recent development of experiments by single molecule measurement on biological systems starts revealing molecular fluctuations in chemical reactions with extremely small numbers of molecules[4–12]. This should provide abundant observations on molecular fluctuations in chemical reactions, and will shed new light on this old problem.

The molecular fluctuations in chemical reactions have been studied by chemical master equations for the distribution function of molecular numbers of each chemical species[1–3]. For spatially homogeneous systems, transition probabilities of molecular reactions are given by a function of molecular concentrations with a coefficient proportional to the system size Ω . In the large Ω limit, Kramers-Moyal expansion[13, 14] of the chemical master equation gives the Fokker-Planck equation, where the molecular fluctuation effects are represented by the generalized diffusion term of the order of $1/\Omega$. Using the analogy between the Fokker-Planck equation and the Schrödinger equation, the Hamilton-Jacobi formalism has been employed to obtain the distribution function in terms of the potential function[15, 16], and there have been attempts to solve this equations using the $1/\Omega$ expansion[17–19] and the Mori-Zwanzig projection method[20, 21].

Gaspard has developed the method to calculate the correlation time of chemical oscillators[22–24]. With his formalism, the probability distribution for the molecular numbers can be obtained for a non-stationary state by solving corresponding Hamilton’s canonical equations. In this work, we further develop the formalism to obtain an explicit expression for the distribution functions in general situations including the case of chemical oscillations.

The paper is organized as follows. In Sec. II, we review the Hamilton-Jacobi formalism

for the chemical master equation to establish the notations, then in Sec. III our main result is derived, i.e. the fundamental solution for the Fokker-Planck equation in the Gaussian approximation. In Sec. IV, a simple method for numerical evaluation of the formula is devised, and the formula is examined in the situation of a steady state and that of an oscillatory state. It is shown that our formula reduces to the one by the linear noise approximation in the case of steady states. In Sec. V, taking the Brusselator as an example, the formulas are evaluated numerically and compared with the results of Monte Carlo simulations. The concluding remarks are given in Sec. VI. Detailed derivations of some of the results are presented in Appendices.

II. FORMULATION

We review the Hamilton-Jacobi method for the chemical master equation to establish the notation, basically following the formalism by Gaspard[23].

A. Molecular fluctuation in chemical reactions

Consider the system that contains d chemical species denoted by X_i ($i = 1, 2, \dots, d$), among which r chemical reactions are taking place:

$$\sum_{i=1}^d \nu_{\rho-}^i X_i \rightarrow \sum_{i=1}^d \nu_{\rho+}^i X_i \quad (\rho = 1, 2, \dots, r), \quad (1)$$

where $\nu_{\rho\pm}^i$ are integers. Thus, the number of i 'th molecule X_i changes by the ρ 'th reaction event as

$$X_i \rightarrow X_i + \Delta X_{\rho}^i \quad (2)$$

with the stoichiometric coefficient $\Delta X_{\rho}^i \equiv \nu_{\rho+}^i - \nu_{\rho-}^i$. In order that a steady chemical oscillation be possible, the system needs steady input and output flows, which may also be included in Eq. (1) as the form of chemical reactions.

Let Ω be the system volume. Then the transition rate W_{ρ} of the reaction ρ may be given by

$$W_{\rho}(\mathbf{X}) = k_{\rho} \Omega \prod_{i=1}^d \prod_{m=1}^{\nu_{\rho-}^i} \frac{X_i - m + 1}{\Omega}, \quad (3)$$

with the reaction constant k_ρ , assuming the system is spatially homogeneous. Then, the master equation for the probability distribution of the molecular numbers $P(\mathbf{X}, t)$ is given by

$$\frac{d}{dt}P(\mathbf{X}, t) = \sum_{\rho=1}^r \left[W_\rho(\mathbf{X} - \Delta\mathbf{X}_\rho)P(\mathbf{X} - \Delta\mathbf{X}_\rho, t) - W_\rho(\mathbf{X})P(\mathbf{X}, t) \right]. \quad (4)$$

B. Chemical Fokker-Planck equation

In the large Ω limit, this can be approximated as the chemical Fokker-Planck equation for the concentration distribution function

$$P(\mathbf{x}, t) \equiv \Omega^{-d}P(\mathbf{X}, t); \quad \mathbf{x} \equiv \frac{\mathbf{X}}{\Omega}. \quad (5)$$

In the lowest order of Ω , the Fokker-Planck equation may be written in the form of

$$\frac{1}{\Omega} \frac{\partial}{\partial t} P(\mathbf{x}, t) = -H \left(\mathbf{x}, \frac{1}{\Omega} \frac{\partial}{\partial \mathbf{x}} \right) P(\mathbf{x}, t) \quad (6)$$

using the ‘‘Hamiltonian’’

$$H(\mathbf{x}, \mathbf{p}) \equiv \sum_i p_i F_i(\mathbf{x}) - \sum_{ij} p_i p_j Q_{ij}(\mathbf{x}), \quad (7)$$

where

$$F_i(\mathbf{x}) \equiv \lim_{\Omega \rightarrow \infty} \frac{1}{\Omega} \sum_{\rho=1}^r \Delta X_\rho^i W_\rho(\Omega \mathbf{x}), \quad (8)$$

$$Q_{ij}(\mathbf{x}) \equiv \lim_{\Omega \rightarrow \infty} \frac{1}{2} \frac{1}{\Omega} \sum_{\rho=1}^r \Delta X_\rho^i \Delta X_\rho^j W_\rho(\Omega \mathbf{x}). \quad (9)$$

The F -term represents the average flow given by the rate equations

$$\frac{d}{dt} \mathbf{x} = \mathbf{F}(\mathbf{x}), \quad (10)$$

while the Q -term represents the diffusion due to the molecular fluctuation around the average motion.

C. Hamilton-Jacobi method

Assuming the form of solution for Eq.(6) as

$$P(\mathbf{x}, t) = \exp [\Omega \phi(\mathbf{x}, t)] \quad (11)$$

with the function $\phi(\mathbf{x}, \mathbf{t})$, we can put the Fokker-Planck equation in the form of Hamilton-Jacobi equation

$$\frac{\partial \phi(\mathbf{x}, t)}{\partial t} + H\left(\mathbf{x}, \frac{\partial \phi(\mathbf{x}, t)}{\partial \mathbf{x}}\right) = 0 \quad (12)$$

in the lowest order of $1/\Omega$.

According to Hamilton-Jacobi theory of classical mechanics, the solution $\phi(\mathbf{x}, t)$ of Eq.(12) gives the position $\mathbf{x}(t)$ and the momentum

$$\mathbf{p}(t) = \frac{\partial \phi(\mathbf{x}, t)}{\partial \mathbf{x}} \quad (13)$$

that satisfy Hamilton's canonical equations of motion

$$\dot{x}_i(t) = \frac{\partial H}{\partial p_i} = F_i(\mathbf{x}) - \sum_j 2Q_{ij}(\mathbf{x})p_j, \quad (14)$$

$$\dot{p}_i(t) = -\frac{\partial H}{\partial x_i} = -\sum_j \frac{\partial F_j(\mathbf{x})}{\partial x_i} p_j + \sum_{j,k} \frac{\partial Q_{jk}(\mathbf{x})}{\partial x_i} p_j p_k. \quad (15)$$

Conversely, the solution of Hamilton-Jacobi equation (12) can be constructed through $\mathbf{x}(t)$ and $\mathbf{p}(t)$ that satisfy Hamilton's canonical equations (14) and (15) as

$$\begin{aligned} \phi(\mathbf{x}, t) &= \int_0^t \left(\sum_i p_i(t') \frac{dx_i(t')}{dt'} - H(\mathbf{x}(t'), \mathbf{p}(t')) \right) dt' + \phi_0(\mathbf{x}_0) \\ &\equiv J(\mathbf{x}_0, \mathbf{p}_0, t) + \phi_0(\mathbf{x}_0), \end{aligned} \quad (16)$$

where $\phi_0(\mathbf{x})$ is the initial condition of $\phi(\mathbf{x}, t)$ at $t = 0$, and \mathbf{x}_0 and $\mathbf{p}_0 = \partial \phi_0 / \partial \mathbf{x}_0$ are the initial values of $\mathbf{x}(t)$ and $\mathbf{p}(t)$ that lead to \mathbf{x} at the time t ; The function $J(\mathbf{x}_0, \mathbf{p}_0, t)$ is the action integral along $\mathbf{x}(t)$ and $\mathbf{p}(t)$ with this initial condition. Note that the rate equation (10) is given by the canonical equation (14) within the $\mathbf{p} = 0$ subspace, where $H = 0$.

III. APPROXIMATE SOLUTION OF HAMILTON-JACOBI EQUATION

We will derive an approximate solution for $\phi(\mathbf{x}, t)$ to obtain a non-equilibrium distribution function (11) in the Gaussian approximation. Suppose that the system starts from a point \mathbf{x}_0^* at time $t = 0$. We take the initial distribution to be Gaussian given by

$$\phi(\mathbf{x}, 0) = \phi_0(\mathbf{x}) = -\frac{1}{2\sigma_0^2}(\mathbf{x} - \mathbf{x}_0^*)^2, \quad (17)$$

and will take the infinitesimal limit of σ_0^2 after we obtain the expression for $\phi(\mathbf{x}, t)$.

Let $\mathbf{x}^*(t)$ be the solution of the rate equation (10) with the initial condition $\mathbf{x}^*(0) = \mathbf{x}_0^*$, then $\mathbf{x}^*(t)$ and $\mathbf{p}^*(t) = 0$ are the solution of Hamilton's canonical equations (14) and (15) with the initial condition

$$\mathbf{x}^*(0) = \mathbf{x}_0^*, \quad \mathbf{p}^*(0) = \left. \frac{\partial \phi(\mathbf{x}, 0)}{\partial \mathbf{x}} \right|_{\mathbf{x}=\mathbf{x}_0^*} = 0. \quad (18)$$

One can see that the maximum of the distribution is always located at $\mathbf{x}^*(t)$ because

$$\left. \frac{\partial \phi(\mathbf{x}, t)}{\partial \mathbf{x}} \right|_{\mathbf{x}=\mathbf{x}^*(t)} = \mathbf{p}^*(t) = 0. \quad (19)$$

We expand $\phi(\mathbf{x}, t)$ around this maximum point $\mathbf{x} = \mathbf{x}^*(t)$ as

$$\begin{aligned} \phi(\mathbf{x}, t) &\approx \phi(\mathbf{x}^*(t), t) + \frac{1}{2} \sum_{i,j} \left. \frac{\partial^2 \phi}{\partial x_i \partial x_j} \right|_* (x_i - x_i^*(t))(x_j - x_j^*(t)) \\ &\equiv -\frac{1}{2} \sum_{i,j} \hat{M}_{ij}^{-1}(t) (x_i - x_i^*(t))(x_j - x_j^*(t)), \end{aligned} \quad (20)$$

where $|_*$ denotes that the derivative is evaluated at $\mathbf{x} = \mathbf{x}^*(t)$. Note that $\phi(\mathbf{x}^*, t) = 0$ from Eq.(16) because $\mathbf{p}^* = 0$ thus $H(\mathbf{x}^*, \mathbf{p}^*) = 0$. Then, the distribution function is written as

$$P(\mathbf{x}, t | \mathbf{x}_0^*) = \left(\frac{\Omega}{2\pi} \right)^{d/2} \frac{1}{\sqrt{|\hat{M}(t)|}} \exp \left[-\frac{\Omega}{2} (\mathbf{x} - \mathbf{x}^*(t))^T \hat{M}(t)^{-1} (\mathbf{x} - \mathbf{x}^*(t)) \right] \quad (21)$$

within Gaussian approximation, and the variances are obtained by

$$\langle (x_i - x_i^*)(x_i - x_j^*) \rangle \equiv \int d\mathbf{x} (x_i - x_i^*)(x_i - x_j^*) P(\mathbf{x}, t | \mathbf{x}_0^*) = \frac{1}{\Omega} \hat{M}_{ij}(t), \quad (22)$$

using the matrix \hat{M} defined by Eq.(20).

Note that Eq.(21) represents the conditional probability distribution, i.e. the fundamental solution of the Fokker-Planck equation with the initial distribution localized at $\mathbf{x} = \mathbf{x}_0^*$. We will derive a compact expression of the covariance matrix $\hat{M}(t)$ in the following.

A. Expansion around the rate equation orbit $\mathbf{x}^*(t)$

The expansion coefficient of Eq.(20) may be written as

$$-\hat{M}_{ij}^{-1}(t) = \left. \frac{\partial^2 \phi(\mathbf{x}, t)}{\partial x_i \partial x_j} \right|_* = \left. \frac{\partial p_j(\mathbf{x}_0(\mathbf{x}, t), t)}{\partial x_i} \right|_*, \quad (23)$$

where $p_j(\mathbf{x}_0, t)$ denotes the j -th component of the momentum at t from the initial condition $(\mathbf{x}_0, \mathbf{p}_0)$ with $\mathbf{p}_0 = \partial \phi_0 / \partial \mathbf{x}|_{\mathbf{x}=\mathbf{x}_0}$. Conversely, the initial position \mathbf{x}_0 can be denoted by

$\mathbf{x}_0(\mathbf{x}, t)$ as a function of the ending point \mathbf{x} at which the solution of Hamilton's equations arrives at the time t . Note that the momentum \mathbf{p} is always related to \mathbf{x} by Eq.(13).

In order to evaluate Eq.(23), we will consider the linear expansion of Hamilton's equations (14) and (15) around the rate equation orbit $(\mathbf{x}^*(t), 0)$:

$$\delta\dot{\mathbf{x}}(t) = \hat{L}(t)\delta\mathbf{x}(t) - 2\hat{Q}(t)\delta\mathbf{p}(t), \quad (24)$$

$$\delta\dot{\mathbf{p}}(t) = -\hat{L}^\dagger(t)\delta\mathbf{p}(t), \quad (25)$$

where $(\delta\mathbf{x}(t), \delta\mathbf{p}(t)) \equiv (\mathbf{x}(t) - \mathbf{x}^*(t), \mathbf{p}(t))$. The matrix $\hat{L}(t)$ and $\hat{Q}(t)$ are defined as

$$L_{ij}(t) \equiv \left. \frac{\partial F_i}{\partial x_j} \right|_{\mathbf{x}=\mathbf{x}^*(t)}, \quad Q_{ij}(t) \equiv Q_{ij}(\mathbf{x}^*(t)), \quad (26)$$

and \dagger denotes the transposed matrix. Note that the operator $\hat{L}(t)$ represents the time development of $\delta\mathbf{x}$ within the $\mathbf{p} = 0$ subspace, namely the deviation given within the rate equation (10).

We define the time evolution operator for the deviation within the rate equation, i.e. for $\delta\mathbf{x}(t)$ within the $\delta\mathbf{p} = 0$ subspace,

$$\hat{U}_L(t, t_0) \equiv \mathcal{T} \exp \left[\int_{t_0}^t dt' \hat{L}(t') \right], \quad (27)$$

where \mathcal{T} is the time ordering operator. Then the formal solution of Eqs.(24) and (25) for both $\delta\mathbf{x}$ and $\delta\mathbf{p}$ can be written down as

$$\delta\mathbf{x}(t) = \hat{U}_L(t, 0) \left[\delta\mathbf{x}(0) - 2\hat{\mathcal{Q}}_L(t)\delta\mathbf{p}(0) \right], \quad (28)$$

$$\delta\mathbf{p}(t) = \hat{U}_L^\dagger(0, t)\delta\mathbf{p}(0), \quad (29)$$

where we have introduced the symmetric matrix

$$\hat{\mathcal{Q}}_L(t) \equiv \int_0^t dt' \hat{U}_L(0, t') \hat{Q}(t') \hat{U}_L^\dagger(0, t'). \quad (30)$$

Basic properties of $\hat{U}_L(t, t_0)$ are given in Appendix A.

B. Expression for $\hat{M}(t)$

The initial deviation $\delta\mathbf{p}(0)$ is related to $\delta\mathbf{x}(0)$ through Eqs.(17) and (18) as

$$\delta\mathbf{p}(0) = \left. \frac{\partial \phi_0(\mathbf{x})}{\partial \mathbf{x}} \right|_{\mathbf{x}=\mathbf{x}(0)} = -\frac{1}{\sigma_0^2} \delta\mathbf{x}(0), \quad (31)$$

therefore, Eqs.(28) and (29) become

$$\delta \mathbf{x}(t) = \hat{U}_L(t, 0) \left[1 - 2\hat{\mathcal{Q}}_L(t) \left(-\frac{1}{\sigma_0^2} \right) \right] \delta \mathbf{x}(0), \quad (32)$$

$$\delta \mathbf{p}(t) = \hat{U}_L^\dagger(0, t) \left(-\frac{1}{\sigma_0^2} \right) \delta \mathbf{x}(0), \quad (33)$$

which lead to the relation between $\delta \mathbf{p}(t)$ and $\delta \mathbf{x}(t)$,

$$\begin{aligned} \delta \mathbf{p}(t) &= \hat{U}_L^\dagger(0, t) \left(-\frac{1}{\sigma_0^2} \right) \left[1 - 2\hat{\mathcal{Q}}_L(t) \left(-\frac{1}{\sigma_0^2} \right) \right]^{-1} \hat{U}_L(0, t) \delta \mathbf{x}(t) \\ &\rightarrow -\hat{U}_L^\dagger(0, t) \frac{1}{2} \hat{\mathcal{Q}}_L^{-1}(t) \hat{U}_L(0, t) \delta \mathbf{x}(t) \end{aligned} \quad (34)$$

in the limit of $\sigma_0^2 \rightarrow 0$. Using Eq.(23), we obtain the expression for the covariance matrix

$$\hat{M}^{-1}(t) = \hat{U}_L^\dagger(0, t) \frac{1}{2} \hat{\mathcal{Q}}_L^{-1}(t) \hat{U}_L(0, t), \quad (35)$$

or

$$\hat{M}(t) = \hat{U}_L(t, 0) 2\hat{\mathcal{Q}}_L(t) \hat{U}_L^\dagger(t, 0). \quad (36)$$

Note that the covariance matrix satisfies

$$\frac{d}{dt} \hat{M}(t) = \hat{L}(t) \hat{M}(t) + \hat{M}(t) \hat{L}^\dagger(t) + 2\hat{Q}(t) \quad (37)$$

with the initial condition $\hat{M}(0) = 0$. This equation has been obtained by the $1/\Omega$ expansion of fluctuation[17].

IV. DISTRIBUTION FUNCTIONS

The major result of this paper is the expression of the covariance matrix (36) for the probability distribution (21), which holds in general transient situations as long as the Gaussian approximation is valid. In this section, first we discuss the numerical method to estimate our formulas, then we will examine this result for two cases: the case where the rate equation leads to a stationary state, and the case where the rate equation gives rise to a stable oscillation.

A. Numerical estimate of the formulas

At this point, it is convenient to introduce the bra and ket notation for the row and column vectors, with which Eqs.(28) and (29) are expressed as

$$|\delta x(t)\rangle = \hat{U}_L(t, 0) \left[|\delta x(0)\rangle - 2\hat{\mathcal{Q}}_L(t) |\delta p(0)\rangle \right], \quad (38)$$

$$\langle \delta p(t) | = \langle \delta p(0) | \hat{U}_L(0, t). \quad (39)$$

The components of the covariance matrix $\hat{M}(t)$ of Eq.(36) and $\hat{\mathcal{Q}}_L(t)$ of Eq.(30) can be numerically estimated easily by solving these equations with proper initial conditions. Let us first introduce the following notations for the solutions of Eqs.(38) and (39):

$$|\delta_x x(t; \delta x_0)\rangle \equiv \hat{U}_L(t, 0) |\delta x_0\rangle, \quad (40)$$

$$|\delta_p x(t; \delta p_0)\rangle \equiv -\hat{U}_L(t, 0) 2\hat{\mathcal{Q}}_L(t) |\delta p_0\rangle, \quad (41)$$

$$\langle \delta p(t; \delta p_0) | \equiv \langle \delta p_0 | \hat{U}_L(0, t). \quad (42)$$

Eq.(40) may be interpreted as the deviation of \mathbf{x} from \mathbf{x}^* by the rate equation with the initial deviation $\delta \mathbf{x}_0$ within the $\mathbf{p} = 0$ subspace. Eqs.(41) and (42) are the deviation of \mathbf{x} and \mathbf{p} , respectively, with the initial deviation $\delta \mathbf{p}_0$. They can be obtained numerically by solving Eqs.(24) and (25) with the initial conditions $(\delta \mathbf{x}, \delta \mathbf{p}) = (\delta \mathbf{x}_0, 0)$ or $(\delta \mathbf{x}, \delta \mathbf{p}) = (0, \delta \mathbf{p}_0)$ at $t = 0$.

Let \hat{I} be the identity matrix and this may be expressed as

$$\hat{I} = \sum_{\alpha} |\alpha\rangle \langle \alpha| \quad (43)$$

by a complete set of orthonormal base vectors $|\alpha\rangle$. Then, a matrix element $\langle i | \hat{M}(t) | j \rangle$ of Eq.(36) can be put in the form

$$\begin{aligned} \langle i | \hat{M}(t) | j \rangle &= \sum_{\alpha} \langle i | \hat{U}_L(t, 0) 2\hat{\mathcal{Q}}_L(t) |\alpha\rangle \langle \alpha | \hat{U}_L^\dagger(t, 0) | j \rangle \\ &= \sum_{\alpha} -\langle i | \delta_p x(t; \alpha) \rangle \langle \delta_x x(t; \alpha) | j \rangle, \end{aligned} \quad (44)$$

where $\langle \delta_x x(t; \alpha) |$ is a transposed column vector of $|\delta_x x(t; \alpha)\rangle$. Similarly, the matrix elements of $\hat{\mathcal{Q}}_L(t)$ can be expressed as

$$\begin{aligned} \langle i | 2\hat{\mathcal{Q}}_L(t) | j \rangle &= \langle i | \hat{U}_L(0, t) \hat{U}_L(t, 0) 2\hat{\mathcal{Q}}_L(t) | j \rangle \\ &= -\langle \delta p(t; i) | \delta_p x(t; j) \rangle. \end{aligned} \quad (45)$$

With these formulas, we can evaluate the matrix elements numerically simply by solving the ODE's, i.e. Eqs.(24) and (25) with proper initial conditions.

B. Fluctuations around the steady state

In the simple case where the rate equation leads to a stationary state \mathbf{x}_s^* , we show that Eq.(36) results in the expressions that have been obtained by the linear noise approximation for the Fokker-Planck equation.

In this case, the matrices $\hat{L}(t)$ and $\hat{Q}(t)$ of Eq.(26) converge to time-independent ones as the rate equation solution $\mathbf{x}^*(t)$ does,

$$\lim_{t \rightarrow \infty} \mathbf{x}^*(t) = \mathbf{x}_s^*, \quad \lim_{t \rightarrow \infty} \hat{L}(t) \equiv \hat{L}_s, \quad \lim_{t \rightarrow \infty} \hat{Q}(t) \equiv \hat{Q}_s, \quad (46)$$

therefore, the fluctuation distribution $P_s(\mathbf{x})$ around the steady state is given by

$$P_s(\mathbf{x}) = \left(\frac{\Omega}{2\pi} \right)^{d/2} \frac{1}{\sqrt{|\hat{M}_s|}} \exp \left[-\frac{\Omega}{2} (\mathbf{x} - \mathbf{x}_s^*)^T \hat{M}_s^{-1} (\mathbf{x} - \mathbf{x}_s^*) \right] \quad (47)$$

with the covariance matrix \hat{M}_s determined by

$$\hat{L}_s \hat{M}_s + \hat{M}_s \hat{L}_s^\dagger + 2\hat{Q}_s = 0 \quad (48)$$

because the covariance matrix should satisfies Eq.(37). The time correlation of fluctuation around the steady state is obtained as

$$\begin{aligned} & \left\langle (\mathbf{x}(t) - \mathbf{x}_s^*) (\mathbf{x}(0) - \mathbf{x}_s^*)^T \right\rangle \\ &= \int \left[\left(\int (\mathbf{x}_t - \mathbf{x}_s^*) P(\mathbf{x}_t, t | \mathbf{x}_0) d\mathbf{x}_t \right) (\mathbf{x}_0 - \mathbf{x}_s^*)^T P_s(\mathbf{x}_0) \right] d\mathbf{x}_0 \\ &= \int (\mathbf{x}^*(t) - \mathbf{x}_s^*) (\mathbf{x}_0 - \mathbf{x}_s^*)^T P_s(\mathbf{x}_0) d\mathbf{x}_0 \\ &= \int \left[e^{\hat{L}_s t} (\mathbf{x}_0 - \mathbf{x}_s^*) \right] (\mathbf{x}_0 - \mathbf{x}_s^*)^T P_s(\mathbf{x}_0) d\mathbf{x}_0 = \frac{1}{\Omega} e^{\hat{L}_s t} \hat{M}_s, \end{aligned} \quad (49)$$

where $t > 0$ and $\mathbf{x}^*(t)$ is the rate equation solution with the initial condition $\mathbf{x}^*(0) = \mathbf{x}_0$. We have used that $\mathbf{x}^*(t) - \mathbf{x}_s^* = e^{\hat{L}_s t} (\mathbf{x}_0 - \mathbf{x}_s^*)$, assuming that $\mathbf{x}^*(t)$ is close to \mathbf{x}_s^* . These expressions are identical to those obtained by the linear noise approximation[3, 25, 26].

C. Fluctuations around the periodic orbit

With our formula (21) with Eq.(35), we can also study the fluctuations around a periodic oscillation. In this subsection, we present analysis on the long time behavior of the distribution around a stable oscillation.

In an autonomous oscillatory system, the distribution relaxes in two ways: the phase diffusion along the periodic orbit and the relaxation within the space perpendicular to the periodic orbit. The distribution diffuses along the periodic orbit because there is no restoring force due to the time translational symmetry; the distribution spreads over the whole orbit after many periods of time. On the other hand, the distribution spreads perpendicular to the orbit to reach a steady form relatively fast. The width of the distribution varies along the orbit, depending on the local stability of the orbit. We study these changes by considering the covariance matrix $\hat{M}(t)$ after many times of the period.

1. Time evolution operator \hat{U} over the period

Let $\mathbf{x}^*(t)$ be the periodic solution for the rate equation (10):

$$\mathbf{x}^*(t + T) = \mathbf{x}^*(t), \quad (50)$$

where T is the period. The initial point on the periodic orbit is denoted by $\mathbf{x}_0^* \equiv \mathbf{x}^*(0)$. Now, we define the time evolution operator \hat{U} around this orbit over the period T ,

$$\hat{U} \equiv \hat{U}_L(T, 0). \quad (51)$$

Note that \hat{U} depends on the starting point $\mathbf{x}^*(0) = \mathbf{x}_0^*$. In this work, we consider only the simplest case where \hat{U} have neither degenerate eigenvalues nor Jordan blocks larger than 1. We describe some of the properties of this operator in this subsection.

The i 'th eigenvalue of \hat{U} is denoted by λ_i and its right and left eigenvectors by $|e_i\rangle$ and $\langle f_i|$, respectively,

$$\hat{U} |e_i\rangle = \lambda_i |e_i\rangle, \quad \langle f_i| \hat{U} = \langle f_i| \lambda_i, \quad (52)$$

with the normalization

$$\langle f_i | e_j \rangle = \delta_{i,j}. \quad (53)$$

For an autonomous system, the largest eigenvalue is 1 and its eigenvectors may be given by

$$\lambda_1 = 1, \quad |e_1\rangle = |F(\mathbf{x}_0^*)\rangle, \quad \langle f_1| = \left. \frac{\partial \langle p^*(0; E)|}{\partial E} \right|_{E=0}. \quad (54)$$

Here, $\mathbf{p}^*(t; E)$ is the periodic orbit outside the $\mathbf{p} = 0$ plane, where the value of the Hamiltonian (7) is non-zero, $E \neq 0$ (see Appendix B). The absolute values of other eigenvalues are smaller than 1 because the periodic orbit is stable. For the simplest case we are considering now, \hat{U} can be expressed as

$$\hat{U} = \sum_i |e_i\rangle \lambda_i \langle f_i|. \quad (55)$$

Now, we define

$$|e_i(t)\rangle \equiv \hat{U}_L(t, 0) |e_i\rangle, \quad \langle f_i(t)| \equiv \langle f_i| \hat{U}_L(0, t), \quad (56)$$

then it is easy to show that they are the right and the left eigenvectors of the time evolution operator $\hat{U}_L(T + t, t)$ over the period at $\mathbf{x}^*(t)$, i.e.,

$$\hat{U}_L(T + t, t) |e_i(t)\rangle = \lambda_i |e_i(t)\rangle, \quad \langle f_i(t)| \hat{U}_L(T + t, t) = \lambda_i \langle f_i(t)|, \quad (57)$$

and

$$\langle f_i(t)|e_j(t)\rangle = \delta_{ij}, \quad (58)$$

with

$$|e_i(T)\rangle = \lambda_i |e_i\rangle, \quad \langle f_i(T)| = \frac{1}{\lambda_i} \langle f_i|. \quad (59)$$

With these notations, we have the expression

$$\hat{U}_L(t, 0) = \sum_\ell |e_\ell(t)\rangle \langle f_\ell|. \quad (60)$$

2. Phase diffusion and period fluctuation

Now, we can obtain the expression for the phase diffusion along the periodic orbit. The unit tangential vector $\hat{\mathbf{n}}_\parallel$ of the periodic orbit at $\mathbf{x}^*(t)$ is given as a function of time by

$$\hat{\mathbf{n}}_\parallel(t) \equiv \frac{\mathbf{F}(\mathbf{x}^*(t))}{|\mathbf{F}(\mathbf{x}^*(t))|} \quad (61)$$

Thus the spatial variance of the orbit in the tangential direction $\langle \Delta x_\parallel^2(t) \rangle$ is obtained from

$$\begin{aligned} \langle \Delta x_\parallel^2(t) \rangle &= \frac{1}{\Omega} \langle \hat{\mathbf{n}}_\parallel(t) | \hat{M}(t) | \hat{\mathbf{n}}_\parallel(t) \rangle \\ &= \frac{1}{\Omega} \frac{1}{|\mathbf{F}(\mathbf{x}^*(t))|^2} \langle F(\mathbf{x}^*(t)) | \hat{M}(t) | F(\mathbf{x}^*(t)) \rangle \end{aligned} \quad (62)$$

in the bracket notation.

Let $\langle (\Delta t_{\mathbf{x}^*(t)})^2 \rangle$ be the variance of the time when each sample passes through the plane perpendicular to the orbit at $\mathbf{x}^*(t)$, then up to the lowest order in Ω , this can be estimated by $\langle \Delta x_{\parallel}^2(t) \rangle$ divided by the square of the average speed,

$$\begin{aligned} \langle (\Delta t_{\mathbf{x}^*(t)})^2 \rangle &= \frac{1}{|\mathbf{F}(\mathbf{x}^*(t))|^2} \langle \Delta x_{\parallel}^2(t) \rangle \\ &= \frac{1}{\Omega} \frac{1}{|\mathbf{F}(\mathbf{x}^*(t))|^4} \langle F(\mathbf{x}^*(t)) | \hat{M}(t) | F(\mathbf{x}^*(t)) \rangle. \end{aligned} \quad (63)$$

Using this expression, we define the period fluctuation $\langle \Delta T^2 \rangle$ by

$$\langle \Delta T^2 \rangle \equiv \lim_{r \rightarrow \infty} \frac{1}{r} \langle \Delta t_{\mathbf{x}^*(rT)}^2 \rangle \quad (64)$$

where r is an integer. We obtain the compact expression

$$\langle \Delta T^2 \rangle = \frac{1}{\Omega} \langle f_1 | 2\hat{\mathcal{Q}}_L(T) | f_1 \rangle. \quad (65)$$

The detailed derivation is given in Appendix C.

3. Distribution perpendicular to the periodic orbit

Let $\hat{\mathbf{n}}_{\perp,i}(t)$ ($2 \leq i \leq d$) be the unit vectors perpendicular to the periodic orbit at $\mathbf{x}^*(t)$ for $0 \leq t < T$. Note that these vectors are in the space spanned by the left eigenvectors $\mathbf{f}_i(t)$ ($2 \leq i \leq d$) of $\hat{U}_L(T+t, t)$, whose eigenvalues are smaller than 1. The variances in the normal space at $\mathbf{x}^*(t)$ for the steady distribution are given by

$$\begin{aligned} \langle \Delta x_{\perp,i}(t) \Delta x_{\perp,j}(t) \rangle_{\infty} &\equiv \lim_{r \rightarrow \infty} \frac{1}{\Omega} \langle \hat{\mathbf{n}}_{\perp,i}(t) | \hat{M}(rT+t) | \hat{\mathbf{n}}_{\perp,j}(t) \rangle \\ &= \frac{1}{\Omega} \sum_{\ell,k=2}^d \langle \hat{\mathbf{n}}_{\perp,i}(t) | e_{\ell}(t) \rangle \left[\frac{\lambda_{\ell} \lambda_k}{1 - \lambda_{\ell} \lambda_k} \langle f_{\ell} | 2\hat{\mathcal{Q}}_L(T) | f_k \rangle + \langle f_{\ell} | 2\hat{\mathcal{Q}}_L(t) | f_k \rangle \right] \langle e_k(t) | \hat{\mathbf{n}}_{\perp,j}(t) \rangle \end{aligned} \quad (66)$$

In the case $|\lambda_2| \gg |\lambda_3|$, the terms with λ_i for $i \geq 3$ can be neglected, thus we obtain the approximate expression

$$\begin{aligned} \langle \Delta x_{\perp,i}(t) \Delta x_{\perp,j}(t) \rangle_{\infty} &\approx \\ \frac{1}{\Omega} \langle \hat{\mathbf{n}}_{\perp,i}(t) | e_2(t) \rangle &\left[\frac{\lambda_2^2}{1 - \lambda_2^2} \langle f_2 | 2\hat{\mathcal{Q}}_L(T) | f_2 \rangle + \langle f_2 | 2\hat{\mathcal{Q}}_L(t) | f_2 \rangle \right] \langle e_2(t) | \hat{\mathbf{n}}_{\perp,j}(t) \rangle. \end{aligned} \quad (67)$$

ρ	Reactions	ΔX_ρ	ΔY_ρ	transition rates W_ρ	w_ρ
1	$\xrightarrow{k_1} X$	1	0	$k_1\Omega$	k_1
2	$X \xrightarrow{k_2} Y$	-1	1	k_2X	k_2x
3	$2X + Y \xrightarrow{k_3} 3X$	1	-1	$k_3 \frac{X(X-1)Y}{\Omega^2}$	k_3x^2y
4	$X \xrightarrow{k_4}$	-1	0	k_4X	k_4x

TABLE I. Reaction table for Brusselator.

This means that the distribution extends in the direction of $\mathbf{e}_2(t)$ projected on the normal space. In the case of two-variable system, i.e. $d = 2$, Eq. (66) becomes simple because there is only one normal vector $\hat{\mathbf{n}}(t) \parallel \mathbf{f}_2(t)$; the variance perpendicular to the orbit is given by

$$\langle (\Delta x_\perp^2(t)) \rangle_\infty = \frac{1}{\Omega} \frac{1}{\langle f_2(t) | f_2(t) \rangle} \left[\frac{\lambda_2^2}{1 - \lambda_2^2} \langle f_2 | 2\hat{\mathcal{Q}}_L(T) | f_2 \rangle + \langle f_2 | 2\hat{\mathcal{Q}}_L(t) | f_2 \rangle \right]. \quad (68)$$

V. NUMERICAL RESULTS FOR BRUSSELTATOR

We numerically evaluate our formulas for Brusselator[27], i.e. a simple model of the chemical oscillation with two chemical species, X and Y (Table I). From Eqs.(8) and (9), F_i and Q_{ij} in the Hamiltonian are given by

$$F_x = k_1 - k_2x + k_3x^2y - k_4x, \quad (69)$$

$$F_y = k_2x - k_3x^2y, \quad (70)$$

$$Q_{xx} = \frac{1}{2}(k_1 + k_2x + k_3x^2y + k_4x) \quad (71)$$

$$Q_{xy} = Q_{yx} = -\frac{1}{2}(k_2x + k_3x^2y) \quad (72)$$

$$Q_{yy} = \frac{1}{2}(k_2x + k_3x^2y). \quad (73)$$

The function $L_{ij}(t)$ defined by Eq.(26) are given by

$$L_{xx}(t) = -k_2 + 2k_3 x^*(t) y^*(t) - k_4, \quad (74)$$

$$L_{xy}(t) = k_3 x^*(t)^2, \quad (75)$$

$$L_{yx}(t) = k_2 - 2k_3 x^*(t) y^*(t), \quad (76)$$

$$L_{yy}(t) = -k_3 x^*(t)^2, \quad (77)$$

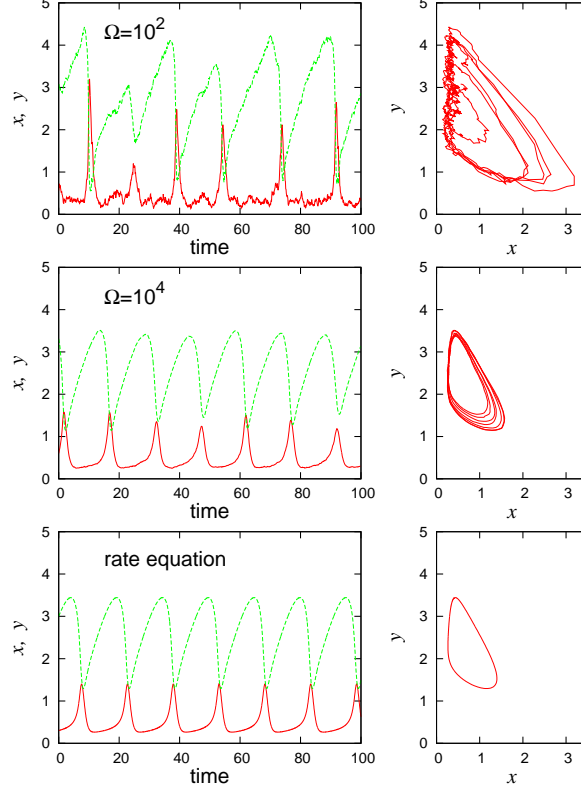


FIG. 1. Time sequences of Brusselator for $\Omega = 100$ (top), 10,000 (middle), and the periodic rate equation solution (bottom). In the left panels, the concentrations x and y are plotted by the red and the green lines respectively as a function of time. In the right panels, the trajectories are plotted in the $x - y$ plane. The parameters for the system are $k_1 = 0.5$, $k_2 = 1.5$, $k_3 = 1.0$, $k_4 = 1.0$, for which the period of the rate equation solution is $T = 15.1631$.

where $(x^*(t), y^*(t))$ is a rate equation solution. The covariance matrix $\hat{M}(t)$ of Eq.(36) is evaluated through Eq.(44) by solving Eqs.(24) and (25) numerically with proper initial conditions. We also performed Monte Carlo simulations to simulate the original master equation (4) using the event driven algorithm.

Figure 1 shows time sequences of the concentrations x and y in sample trajectories for $\Omega = 100$ and 10,000 along with the periodic rate equation solution. The molecular fluctuation is large in the smaller system.

Figure 2 shows the time development of the ensemble of 10,000 data points generated by Monte Carlo simulations along with the ellipses given by the covariance matrix as

$$(\mathbf{x} - \mathbf{x}^*(t))^T \hat{M}(t)^{-1} (\mathbf{x} - \mathbf{x}^*(t)) = \frac{4}{\Omega} \quad (78)$$

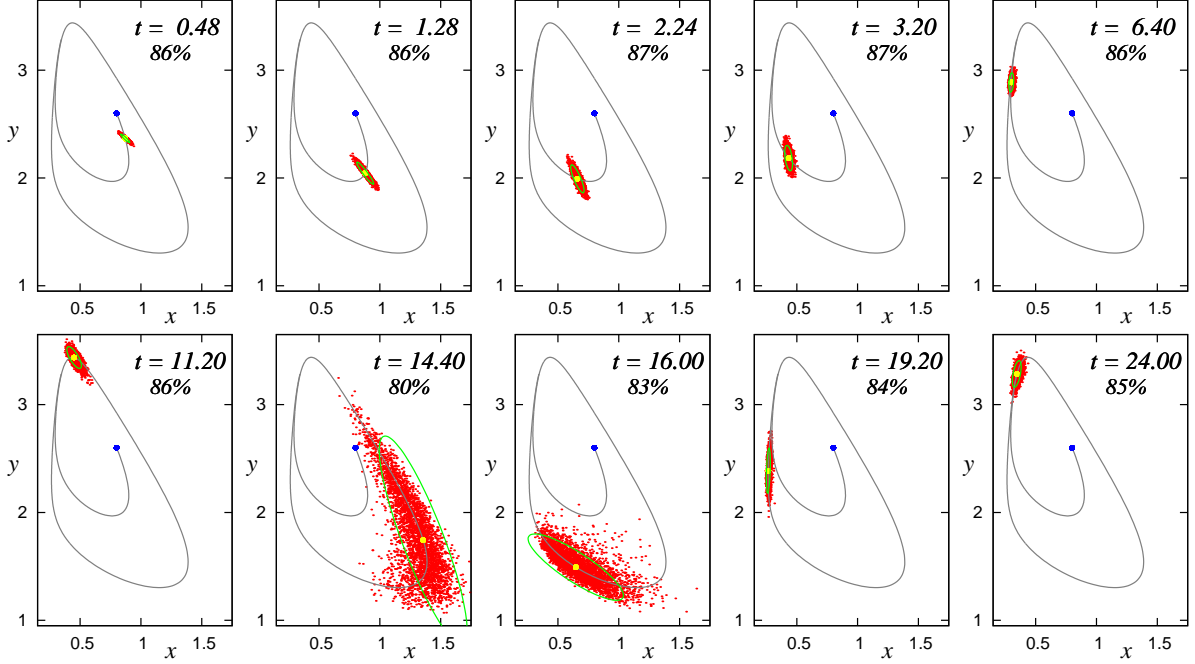


FIG. 2. Time development of distribution for Brusselator. 10,000 samples of Monte Carlo simulations are plotted by the red dots along with the covariance matrix \hat{M} estimated by Eq.(44) ; \hat{M} 's are represented by the green ellipses given by $\delta\mathbf{x}^T \hat{M}^{-1} \delta\mathbf{x} = 4/\Omega$, where $\delta\mathbf{x}^T \equiv (x - x^*(t), y - y^*(t))$. The percentages of the samples that fall within the ellipses are shown in each panel. The gray curves represent the trajectory by the rate equation starting from the initial point marked by the blue circles. The system parameters are $k_1 = 0.5$, $k_2 = 1.5$, $k_3 = 1.0$, $k_4 = 1.0$, and $\Omega = 10^4$. The initial point is $(x_0^*, y_0^*) = (0.8, 2.6)$.

with $\Omega = 10^4$. The initial point is marked by a blue circle and the rate equation trajectory is shown by a gray curve in each plot. One can see that the data point distributions obtained by Monte Carlo simulations are fairly well represented by the ellipses. The percentages of the samples that fall within the ellipse are shown in each plots; Except for a few cases where the distribution is near the curving parts of the trajectory, these percentages are close to 87%, i.e., the percentage for the two-dimensional Gaussian distribution. The distribution extends initially transversely across the trajectory, but eventually along the periodic orbit. The distribution returns to the Gaussian in the slow moving part of the trajectory even after it deviates substantially from the Gaussian around the turning points in the fast moving part.

The expression of period fluctuation (65) is examined by the relaxation time τ in the

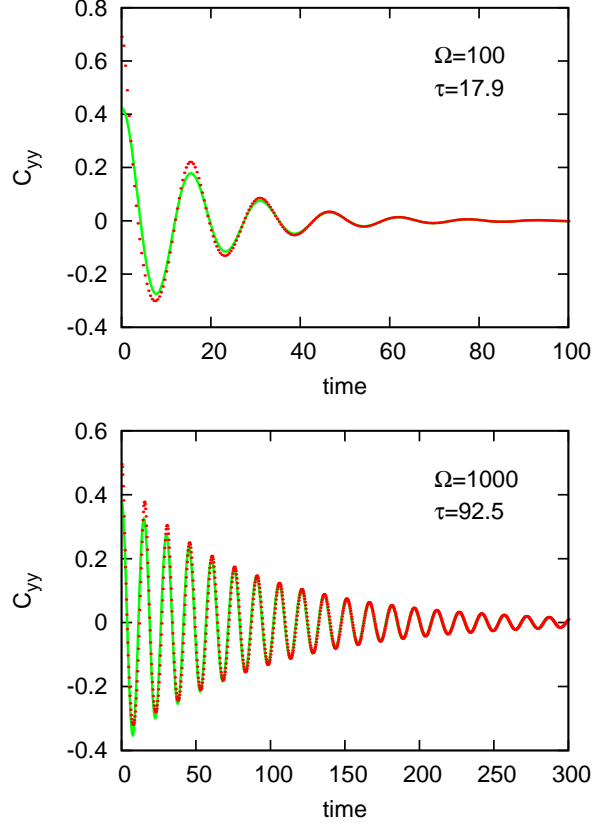


FIG. 3. Correlation functions $C_{yy}(t)$. The dotted lines are the results of Monte Carlo simulations and the green lines are fitting functions by Eq.(80) to estimate the relaxation time τ . $\Omega = 100$ (the upper panel) and 1000 (the lower panel) and the rest of the parameters are the same with those for Figs. 1 and 2.

correlation function for the y variable

$$C_{yy}(t) \equiv \lim_{T_{\text{av}} \rightarrow \infty} \frac{1}{T_{\text{av}}} \int_0^{T_{\text{av}}} \left[\langle y(t+t_0)y(t_0) \rangle - \langle y(t+t_0) \rangle \langle y(t_0) \rangle \right] dt_0. \quad (79)$$

From simple calculation[23], the correlation function is expected to decay as

$$C_{yy}(t) \sim Ae^{-t/\tau} \cos(\omega t) \quad (80)$$

with the relaxation time

$$\tau = \frac{T^3}{2\pi^2 \langle \Delta T^2 \rangle} = \Omega \frac{T^3}{2\pi^2 \langle f_1 | 2\hat{Q}_L(T) | f_1 \rangle}. \quad (81)$$

Figure 3 shows the correlation functions obtained by Monte Carlo simulations (the red dotted lines) and the fitting functions (80) (the green lines) for $\Omega = 100$ and 1,000. The relaxation

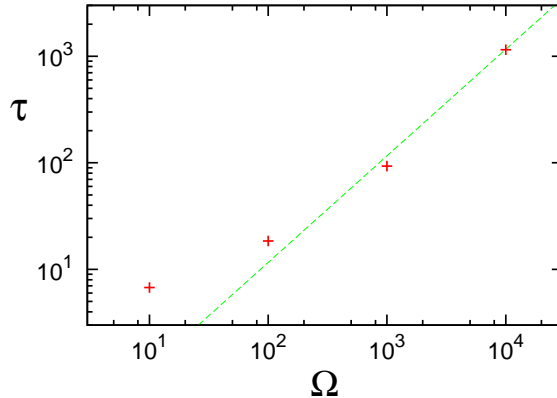


FIG. 4. Correlation time vs. Ω . The red crosses shows the relaxation times estimated by the Monte Carlo simulations, and the green dashed line shows the line by Eq.(81). The parameters are the same with those for Figs. 1 and 2, for which $T = 15.1631$ and $\langle f_1 | 2\hat{Q}_L(T) | f_1 \rangle = 1519.29$.

times obtained by the fitting are plotted in Fig.4 by the red crosses vs. Ω with the estimate by Eq.(81) (the green dashed line). They agree well for $\Omega \gtrsim 100$.

The variance of the distribution width (68) perpendicular to the periodic orbit is shown by the green band in Fig.5 with the dots that represents the ensemble of 10,000 samples by Monte Carlo simulations in the steady state. The width of the green band represents well the local width of the distribution of the Monte Carlo simulations.

VI. CONCLUDING REMARKS

Using Hamilton-Jacobi method, we have derived a compact formula for the conditional probability distribution by solving the chemical Fokker-Planck equation within the Gaussian approximation. The formula is quite general and given for an arbitrary initial value of \mathbf{x}_0 ; it can be applied not only to stationary states but also to oscillatory states and transient processes. In the case of stationary states, the formula reduces to the one obtained by the linear noise approximation[3, 25, 26]. In the case of oscillatory states, we have derived the expressions for the phase diffusion along the stable periodic orbit and for the steady distribution in the space perpendicular to the periodic orbit. We also have developed the method to evaluate these expressions numerically. Taking the Brusselator as an example, we have estimated the formulas numerically and compared them with the results of the Monte Carlo simulations; They agree quite well.

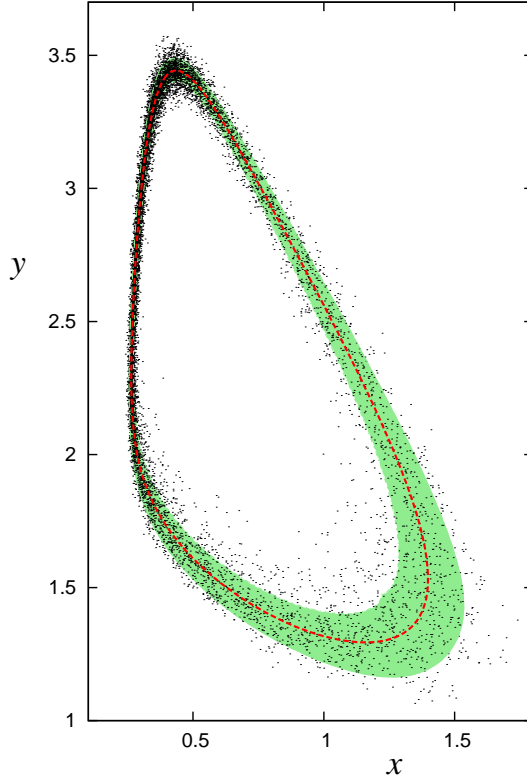


FIG. 5. Steady state distribution. The red dashed line represents the periodic orbit by the rate equation, and the green area around it shows the region within the distance of the square root of the local variance Eq.(68) from the rate equation orbit. The dots show 10,000 samples by the Monte Carlo simulations. $\Omega = 10,000$ and the rest of the parameters are the same with those for Figs. 1 and 2.

The present theory is based on the Hamilton-Jacobi formalism developed by Gaspard[23], but the actual distribution functions that we obtained are different; Gaspard expanded the distribution function by the time variable, but we obtained the expression for the distribution function by expanding by the x variables at a given time t . Applying our formula for the periodic orbit, we obtain the expressions for both phase diffusion along the orbit and the steady distribution in the space perpendicular to the orbit. The phase diffusion is directly related to the temporal fluctuation, and the expression for the period variance is derived. Our expression for the period variance is apparently different from the one by Gaspard[23], but they are shown to be equivalent.

Expressions equivalent to some of our results have been obtained using slightly different method of expansion[17, 19, 25]. Although we kept only the lowest order of $1/\Omega$ in the

fluctuations with the Gaussian approximation, our method is fairly straightforward and the final expression is rather general and yet compact. It also allows simple numerical evaluation.

Appendix A: General Properties of Time evolution operator $\hat{U}_L(t, t_0)$

In this appendix, various properties of the time evolution operator $\hat{U}_L(t, t_0)$ are presented. The time evolution operator (27) is defined as

$$\begin{aligned}\hat{U}_L(t, t_0) &\equiv \mathcal{T} \exp \left[\int_{t_0}^t dt' \hat{L}(t') \right] \\ &\equiv 1 + \int_{t_0}^t dt_1 \hat{L}(t_1) + \int_{t_0}^t dt_1 \int_{t_0}^{t_1} dt_2 \hat{L}(t_1) \hat{L}(t_2) + \cdots \\ &= 1 + \int_{t_0}^t dt_1 \hat{L}(t_1) + \int_{t_0}^t dt_1 \int_{t_1}^t dt_2 \hat{L}(t_2) \hat{L}(t_1) + \cdots ,\end{aligned}\tag{A1}$$

for the both cases of $t \geq t_0$ and $t \leq t_0$. The second equality gives the definition of the time ordering operator \mathcal{T} . From this, it is easy to see that the operator satisfies

$$\frac{d}{dt} \hat{U}_L(t, t_0) = \hat{L}(t) \hat{U}_L(t, t_0),\tag{A2}$$

$$\frac{d}{dt_0} \hat{U}_L(t, t_0) = -\hat{U}_L(t, t_0) \hat{L}(t_0),\tag{A3}$$

$$\hat{U}_L(t_0, t_0) = 1,\tag{A4}$$

and the following equalities hold:

$$\hat{U}_L(t, t_0) = \hat{U}_L(t, t_1) \hat{U}_L(t_1, t_0),\tag{A5}$$

$$\hat{U}_L^{-1}(t, t_0) = \hat{U}_L(t_0, t),\tag{A6}$$

$$\hat{U}_L^\dagger(t, t_0) = \hat{U}_{-L^\dagger}(t_0, t),\tag{A7}$$

$$\left(\hat{U}_L^{-1}(t, t_0) \right)^\dagger = \left(\hat{U}_L^\dagger(t, t_0) \right)^{-1} = \hat{U}_{-L^\dagger}(t, t_0).\tag{A8}$$

Appendix B: Right and Left Eigenvectors for \hat{U}

For the time evolution operator \hat{U} over the period T , the expressions for the right and left eigenvectors, $|e_1\rangle$ and $\langle f_1|$, with the eigenvalue $\lambda_1 = 1$ can be obtained.

It is easy to see that the right eigenvector of λ_1 is given by

$$|e_1\rangle = |F(\mathbf{x}_0^*)\rangle\tag{B1}$$

because from Eqs.(14) and (26)

$$\frac{d}{dt}F_i(\mathbf{x}^*(t)) = L_{ij}(t)F_j(\mathbf{x}^*(t)), \quad (\text{B2})$$

that gives

$$|F(\mathbf{x}_0^*)\rangle = |F(\mathbf{x}^*(T))\rangle = \hat{U} |F(\mathbf{x}_0^*)\rangle. \quad (\text{B3})$$

The corresponding left eigenvector $\langle f_1|$ can be also obtained as follows. Consider the periodic orbit $(\mathbf{x}^*(t; E), \mathbf{p}^*(t; E))$ outside the $\mathbf{p} = 0$ subspace, where the value of Hamiltonian E is non-zero. Suppose that it is an analytic function of E with $(\mathbf{x}^*(t; 0), \mathbf{p}^*(t; 0)) = (\mathbf{x}^*(t), 0)$, and its period is given by $T(E)$ as a function of E .

Let us define the deviations

$$\delta\mathbf{x}^*(t) \equiv \mathbf{x}^*(t; \delta E) - \mathbf{x}^*(t), \quad \delta\mathbf{p}^*(t) \equiv \mathbf{p}^*(t; \delta E) \quad (\text{B4})$$

for small δE . These satisfy Eqs.(24) and (25), thus the formal solutions are given by Eqs.(28) and (29).

Within the first order of δE , $\delta\mathbf{p}^*(0)$ is given by

$$\delta\mathbf{p}^*(0) = \mathbf{p}^*(T(\delta E); \delta E) \approx \mathbf{p}^*(T(0); \delta E) = \delta\mathbf{p}^*(T), \quad (\text{B5})$$

where we have used $\mathbf{p}^*(t; 0) = 0$ and $T(0) = T$. Using the formal solution (29), the last expression is written as

$$\delta\mathbf{p}^*(T) = \hat{U}_L^\dagger(0, T)\delta\mathbf{p}^*(0) = \left(\hat{U}^{-1}\right)^\dagger \delta\mathbf{p}^*(0), \quad (\text{B6})$$

which shows that $\langle \delta\mathbf{p}^*(0)|$ is the left eigenvector in the bracket notation,

$$\langle \delta\mathbf{p}^*(0)| \hat{U} = \langle \delta\mathbf{p}^*(0)|. \quad (\text{B7})$$

From the normalization (53) with the right eigenvector (B1), we have

$$\langle f_1| = \frac{\langle \delta\mathbf{p}^*(0)|}{\delta E} = \frac{\partial \langle \mathbf{p}^*(0; E)|}{\partial E} \Big|_{E=0} \quad (\text{B8})$$

because

$$\delta E = \langle \delta\mathbf{p}^*(0)|F(\mathbf{x}_0^*)\rangle \quad (\text{B9})$$

from Eq.(7) within the lowest order of δE .

Appendix C: Covariance matrix $\hat{M}(t + rT)$ after many periods of T

We derive the expression for the covariance matrix $\hat{M}(rT + t)$ for a large integer r in the case of the periodic orbit $\mathbf{x}^*(t)$ with the period T . With the expression, we obtain Eq.(65) for the period fluctuation and Eq.(66) for the fluctuations perpendicular to the orbit in the steady distribution.

For an integer r and $0 \leq t < T$, we can rewrite Eq.(36) as

$$\begin{aligned}
\hat{M}(rT + t) &= \hat{U}_L(rT + t, 0) 2\hat{\mathcal{Q}}_L(rT + t) \hat{U}_L^\dagger(rT + t, 0) \\
&= \hat{U}_L(rT + t, 0) \left[\int_0^{rT+t} dt' \hat{U}_L(0, t') 2\hat{\mathcal{Q}}(t') \hat{U}_L^\dagger(0, t') \right] \hat{U}_L^\dagger(rT + t, 0) \\
&= \hat{U}_L(rT + t, 0) \left[\sum_{s=0}^{r-1} \int_0^T dt' \hat{U}_L(0, sT + t') 2\hat{\mathcal{Q}}(t') \hat{U}_L^\dagger(0, sT + t') \right. \\
&\quad \left. + \int_0^t dt' \hat{U}_L(0, rT + t') 2\hat{\mathcal{Q}}(t') \hat{U}_L^\dagger(0, rT + t') \right] \hat{U}_L^\dagger(rT + t, 0) \\
&= \hat{U}_L(rT + t, 0) \left[\sum_{s=0}^{r-1} \hat{U}_L(0, sT) \left(\int_0^T dt' \hat{U}_L(0, t') 2\hat{\mathcal{Q}}(t') \hat{U}_L^\dagger(0, t') \right) \hat{U}_L^\dagger(0, sT) \right. \\
&\quad \left. + \hat{U}_L(0, rT) \left(\int_0^t dt' \hat{U}_L(0, t') 2\hat{\mathcal{Q}}(t') \hat{U}_L^\dagger(0, t') \right) \hat{U}_L^\dagger(0, rT) \right] \hat{U}_L^\dagger(rT + t, 0) \\
&= \hat{U}_L(t, 0) \left[\sum_{s=0}^{r-1} \hat{U}^{r-s} 2\hat{\mathcal{Q}}_L(T) \left(\hat{U}^{r-s} \right)^\dagger + 2\hat{\mathcal{Q}}_L(t) \right] \hat{U}_L^\dagger(t, 0) \\
&= \hat{U}_L(t, 0) \left[\sum_{s=1}^r \hat{U}^s 2\hat{\mathcal{Q}}_L(T) \left(\hat{U}^s \right)^\dagger + 2\hat{\mathcal{Q}}_L(t) \right] \hat{U}_L^\dagger(t, 0), \tag{C1}
\end{aligned}$$

where we have used $\hat{\mathcal{Q}}(t + T) = \hat{\mathcal{Q}}(t)$.

For $t = 0$, $\hat{U}_L(t, 0) = 1$ and $\hat{\mathcal{Q}}_L(t) = 0$, thus using the spectral representation Eq.(55) into this, we have

$$\begin{aligned}
\frac{1}{r} \langle e_1 | \hat{M}(rT) | e_1 \rangle &= \frac{1}{r} \sum_{s=1}^r \langle e_1 | \left(\sum_i |e_i\rangle \lambda_i^s \langle f_i| \right) 2\hat{\mathcal{Q}}_L(T) \left(\sum_j |f_j\rangle \lambda_j^s \langle e_j| \right) | e_1 \rangle \\
&\rightarrow \langle e_1 | e_1 \rangle \langle f_1 | 2\hat{\mathcal{Q}}_L(T) | f_1 \rangle \langle e_1 | e_1 \rangle \tag{C2}
\end{aligned}$$

as $r \rightarrow \infty$ because $|\lambda_i| < 1$ for $i \geq 2$. From Eq.(64) with Eq.(B1), this gives

$$\langle \Delta T^2 \rangle = \frac{1}{\Omega} \langle f_1 | 2\hat{\mathcal{Q}}_L(T) | f_1 \rangle, \tag{C3}$$

which is Eq.(65).

The variances to the direction $\mathbf{n}_{\perp,i}(t)$ normal to the orbit at $\mathbf{x}^*(t)$ can be calculated as

$$\begin{aligned}
\langle \Delta x_{\perp,i}(t) \Delta x_{\perp,j}(t) \rangle &= \frac{1}{\Omega} \langle n_{\perp,i}(t) | \hat{M}(t+rT) | n_{\perp,j}(t) \rangle \\
&= \frac{1}{\Omega} \sum_{\ell,k=2}^d \langle n_{\perp,i}(t) | e_{\ell}(t) \rangle \left[\sum_{s=1}^r \lambda_{\ell}^s \langle f_{\ell} | 2\hat{Q}_L(T) | f_k \rangle \lambda_k^s + \langle f_{\ell} | 2\hat{Q}_L(t) | f_k \rangle \right] \langle e_k(t) | n_{\perp,j}(t) \rangle \\
&\xrightarrow{r \rightarrow \infty} \frac{1}{\Omega} \sum_{\ell,k=2}^d \langle n_{\perp,i}(t) | e_{\ell}(t) \rangle \left[\frac{\lambda_{\ell} \lambda_k}{1 - \lambda_{\ell} \lambda_k} \langle f_{\ell} | 2\hat{Q}_L(T) | f_k \rangle + \langle f_{\ell} | 2\hat{Q}_L(t) | f_k \rangle \right] \langle e_k(t) | n_{\perp,j}(t) \rangle,
\end{aligned} \tag{C4}$$

which is Eq.(66). The matrix elements in Eqs.(C3) and (C4) can be numerically estimated by Eq.(45),

$$\langle f_{\ell} | 2\hat{Q}_L(t) | f_k \rangle = - \langle \delta p(t; f_{\ell}) | \delta p x(t; f_k) \rangle. \tag{C5}$$

Appendix D: Equivalence of Eq.(65) with Gaspard's expression

Gaspard[22, 23] has given the correlation time in terms of the energy derivative of the period $T(E)$. We show his expression is equivalent with our expression Eq.(65).

As in Appendix B, the deviation of the periodic orbit $\delta \mathbf{x}^*(t)$ in Eq.(B4) at $t = 0$ is expressed within the lowest order of δE as

$$\begin{aligned}
\delta \mathbf{x}^*(0) &= \mathbf{x}^*(T(\delta E); \delta E) - \mathbf{x}^*(T(0); 0) \\
&\approx \delta \mathbf{x}^*(T(0)) + \mathbf{F}'(\mathbf{x}_0^*) T'(0) \delta E,
\end{aligned} \tag{D1}$$

where $T'(E)$ denotes the E derivative of $T(E)$. Again, using the formal solution (28) with the notation (51), we have

$$\delta \mathbf{x}^*(T) = \hat{U} \left(\delta \mathbf{x}^*(0) - 2\hat{Q}_L(T) \delta \mathbf{p}^*(0) \right) \tag{D2}$$

By inserting this into Eq.(D1) with Eqs.(B1) and (B8), we have

$$(1 - \hat{U}) |\delta x^*(0)\rangle = \left(-\hat{U} 2\hat{Q}_L(T) |f_1\rangle + |e_1\rangle T'(0) \right) \delta E \tag{D3}$$

in the bracket notation. Taking the inner product of this with $\langle f_1 |$, i.e. the left eigenvector of \hat{U} with the eigenvalue 1, this gives

$$T'(0) = \langle f_1 | 2\hat{Q}_L(T) | f_1 \rangle, \tag{D4}$$

therefore, from Eq.(65) we obtain

$$\langle \Delta T^2 \rangle = \frac{1}{\Omega} \frac{\partial T}{\partial E} \Big|_{E=0}. \quad (\text{D5})$$

With Eq.(81), this is equivalent to Gaspard's expression.

-
- [1] C. W. Gardiner, *Handbook of Stochastic Methods for Physics, Chemistry and the Natural Sciences*, 3rd ed. (Springer, 2004).
 - [2] H. Risken, *The Fokker-Planck Equation* (Springer-Verlag, 1984).
 - [3] N. G. van Kampen, *Stochastic processes in physics and chemistry* (Elsevier, 1992).
 - [4] N. Barkai and S. Leibler, *Nature* **403**, 267 (2000).
 - [5] D. Gonze, J. Halloy, and A. Goldbeter, *PNAS* **99**, 673 (2002).
 - [6] H. Hirata, S. Yoshiura, T. Ohtsuka, Y. Bessho, T. Harada, K. Yoshikawa, and R. Kageyama, *Science* **298**, 840 (2002).
 - [7] N. Geva-Zatorsky, N. Rosenfeld, S. Itzkovitz, R. Milo1, A. Sigal, E. Dekel, T. Yarnitzky, Y. Liron, P. Polak, G. Lahav, and U. Alon, *Molecular Systems Biology* **2**, 2006.0033 (2006).
 - [8] M. B. Elowitz and S. Leibler, *Nature* **403**, 335 (2000).
 - [9] M. R. Atkinson, M. A. Savageau, J. T. Myers, and A. J. Ninfa, *Cell* **113**, 597 (2003).
 - [10] M. Tigges, T. T. Marquez-Lago, J. Stelling, and M. Fussenegger, *Nature* **457**, 309 (2009).
 - [11] E. Fung, W. W. Wong, J. K. Suen, T. Bulter, S. Lee, and J. C. Liao, *Nature* **435**, 118 (2005).
 - [12] R. Nishino, T. Sakaue, and H. Nakanishi, *PLoS ONE* **8**, e60938 (2013).
 - [13] H. A. Kramers, *Physica* **7**, 284 (1940).
 - [14] J. E. Moyal, *J. Roy. Stat. Soc.* **B11**, 150 (1949).
 - [15] R. Kubo, K. Matsuo, and K. Kitahara, *J. Stat. Phys.* **9**, 51 (1973).
 - [16] K. Kitahara, *Adv. Chem. Phys.* **29**, 85 (1975).
 - [17] K. Tomita and H. Tomita, *Prog. Theor. Phys.* **51**, 1731 (1974).
 - [18] K. Tomita, T. Ohta, and H. Tomita, *Prog. Theor. Phys.* **52**, 1744 (1974).
 - [19] W. Vance and J. Ross, *J. Chem. Phys.* **105**, 479 (1996).
 - [20] S. Grossmann and R. Schraner, *Z. Physik* **B 30**, 325 (1978).
 - [21] R. Schraner, S. Grossmann, and P. H. Richter, *Z. Physik* **B 35**, 363 (1979).
 - [22] P. Gaspard, *J. Stat. Phys.* **106**, 57 (2002).

- [23] P. Gaspard, J. Chem. Phys. **117**, 8905 (2002).
- [24] D. Gonze, J. Halloy, and P. Gaspard, J. Chem. Phys. **116**, 10997 (2002).
- [25] J. Elf and M. Ehrenberg, Genome Research **13**, 2475 (2003).
- [26] M. Scott, T. Hwa, and B. Ingalls, PNAS **2007**, 7402 (2007).
- [27] I. Prigogine and R. Lefever, J. Chem. Phys. **48**, 1695 (1968).